

Evidence for $\eta' - \pi$ splitting in unquenched lattice QCD

R. Frezzotti, M. Masetti, R. Petronzio

Dipartimento di Fisica, Università di Roma *Tor Vergata*

and

INFN, Sezione di Roma II

Viale della Ricerca Scientifica, 00133 Roma, Italy

May 30, 1996

Abstract

We perform an extrapolation from negative to positive flavour numbers of full QCD lattice estimates of the η' mass. The extrapolations are carried out by keeping ρ and π masses at fixed values. We find an $\eta' - \pi$ splitting which shows a flavour dependence consistent with the Witten Veneziano formula based on the $U(1)$ anomaly. The quantitative splitting is consistent with the estimates made in the quenched approximation.

ROM2F-96-28

1 Introduction

The quenched approximation in lattice QCD appears to reproduce with remarkable accuracy most of the experimental pattern of the hadronic spectrum. Unquenched corrections are small when the comparison with the quenched case is performed at fixed values of the lattice spacing and of the renormalized quark mass. These two parameters can be fixed by keeping two independent physical quantities like the ρ and π masses fixed. The bermion method exploits the smoothness of dynamical flavour dependence studied at fixed renormalized quantities to make estimates in full QCD which are extrapolations of results obtained at negative flavour numbers, where fermions are replaced by “bermions”, i.e. bosons with a fermion action [1]. This procedure has allowed to show the presence of sizeable unquenching effects in light and heavy pseudoscalar decay constants [2]. A quantity where unquenching effects are expected to be dramatic is the η' mass: it is degenerate with the pion mass in the quenched approximation but splits from it in the unquenched case. According to the Witten Veneziano formula

$$m_{\eta'}^2 = m_{\pi}^2 + 3 \frac{n_f}{N_c} m_0^2 \quad (1)$$

where n_f is the number of dynamical fermion flavours, N_c is the number of color and m_0 is related to the topological susceptibility and constant in the limit $\frac{n_f}{N_c} \rightarrow 0$ [3, 4]. For negative flavour numbers the splitting is expected to make the η' lighter than the pion.

In this paper we study the n_f dependence of the η' mass with the bermion method. We find that eq. 1 is verified: the splitting m_0^2 is independent from n_f within the statistical errors and is consistent with the indirect estimate made in the quenched approximation, which instead *assumes* the validity of eq. 1. The correlations of two flavour singlet currents involve two classes of diagrams: those where two quark propagators connect the two currents (the “fish” diagrams) and those which need gluons to be connected (the “eyes” diagrams). In the quenched approximation only the fish diagrams are relevant and they lead to degenerate masses for singlet and non singlet currents. The eyes can be evaluated in the approximation where there are no intermediate quark loops also in the quenched approximation: this was done in [5] by using a modified wall source method. The calculation of the singlet correlations with the bermions provides directly eyes and fishes. The first

part of this paper is devoted to the detailed discussion of the correlations used in the calculations while the second presents our results.

2 The bermion currents

The action for QCD with negative flavour number n_f can be written in terms of $n_b = |n_f|/2$ commuting spinors $\phi_b(x)$ called bermions:

$$S_b^{(n_b)}[U, \phi, \phi^\dagger] = S_G[U] + \sum_{x,y,z} \sum_{i=1}^{n_b} \phi_i^\dagger(x) Q(x, z) Q(z, y) \phi_i(y) \quad (2)$$

where $S_G[U]$ is the gauge action, spin and color indices are implicit and Q is the Wilson discretization of the Dirac operator

$$\begin{aligned} [Q\phi_i](x) &= \frac{1}{2\kappa} \gamma_5 \phi_i(x) - \frac{1}{2} \gamma_5 \sum_{\mu=0}^3 U_\mu(x) (1 - \gamma_\mu) \phi_i(x + \mu) \\ &\quad - \frac{1}{2} \gamma_5 \sum_{\mu=0}^3 U_\mu^\dagger(x - \mu) (1 + \gamma_\mu) \phi_i(x - \mu) \end{aligned} \quad (3)$$

The presence of bermions in the functional integral and in the Monte Carlo simulation allows to measure their correlations directly as averages over the corresponding fields. In addition, different flavours allow to disentangle fish diagrams from eyes and to recombine them in the mixture appropriate for singlet currents correlations.

We have considered the following bermion currents

$$Q_5^{ij}(x) = \phi_i^\dagger(x) \gamma_5 \phi_j(x) \quad (4)$$

$$P_5^{ij}(x) = \sum_y \phi_i^\dagger(y) Q(y, x) \phi_j(x) \quad (5)$$

where i and j are flavour indices. The correlation $\langle P_5^{ii}(x) P_5^{ii}(y) \rangle$ corresponds to the usual fermion correlation with flavour diagonal pseudoscalar currents and receives contributions from fish and eye diagrams. Fish diagrams can be isolated by measuring the correlation of flavour off-diagonal currents

$$G_\pi(x, y) = \langle P_5^{ij}(x) P_5^{ji}(y) \rangle \quad i \neq j \quad (6)$$

and eye diagrams by measuring

$$H(x, y) = \langle P_5^{ii}(x) P_5^{jj}(y) \rangle \quad i \neq j \quad (7)$$

The combination which projects onto the singlet state is:

$$G_{\eta'}(x, y) = G_\pi(x, y) - n_f H(x, y) \quad (8)$$

The same correlations with P_5^{ij} replaced by the pointlike bilinear Q_5^{ij} of eq. 4 get the fermion propagators replaced by bermion propagators, which are the inverse of the square of the Dirac operator Q^2 . Following the technique discussed in [6] these correlations can be shown to be dominated by the same lowest lying states as the P_5 ones. In Appendix A we show that the only pseudoscalar one particle states which contribute to the correlation

$$H_{Q^2}(x, y) = \langle Q_5^{ii}(x) Q_5^{jj}(y) \rangle \quad i \neq j \quad (9)$$

are flavour singlet mesons, and therefore this correlation is dominated at large times by the η' without contaminations from pion states.

In general it is convenient to calculate fish correlations by standard inversion of the Dirac operator with fixed origin, while eyes are obtained only by direct computation of the correlations between bermion bilinears summed over all possible origins. In order to improve the signal of bermion correlations, we have applied different variations of the ‘‘one link integral’’ technique to the bermion field, replacing, whenever possible, a field with its average in the surrounding bermion and gauge configuration. In Appendix B we discuss briefly the method and the relevant formulae.

3 Results

Our simulations are performed on a $16^3 \times 32$ lattice at fixed renormalized π and ρ masses: $m_\pi = 0.46$ and $m_\rho = 0.66$ or $m_\pi = 0.56$ and $m_\rho = 0.71$. We refer to these two cases from the value of the ratio $R_2 = m_\pi^2/m_\rho^2$ which is equal to 0.5 and 0.6 respectively: the smaller its value the closer is the simulation to the classical limit.

The main results of this paper are the evidence for a state lighter than the pion, shown in figure 1 for $R_2 = 0.5$ and $n_f = -4$, and the determination of the parameter m_0 of eq. 1 at different values of R_2 and as a function of

the flavour number. This allows to investigate on further flavour dependence of the η' mass beyond the one already present in the large N_c limit in the Witten Veneziano expression.

The determination of the mass splitting $\Delta m = m_{\eta'} - m_\pi$ can be extracted from the quantity

$$R(t) = -\frac{1}{n_f} \log[G_{\eta'}(t)/G_\pi(t)] = -\frac{1}{n_f} \log[1 - n_f H(t)/G_\pi(t)] \quad (10)$$

which grows linearly with time in the region $0 \ll t \ll \frac{T}{2}$, where T is the total lattice size in the time direction:

$$R(t) \longrightarrow \frac{\Delta m}{n_f} t \quad (11)$$

In the quenched case, by taking the limit $n_f \rightarrow 0$ and by assuming the validity of Witten Veneziano expression, the previous formulae reduce to those used in [5]:

$$R_0(t) = \frac{H(t)}{G_\pi(t)} \longrightarrow \frac{m_0^2}{2m_\pi} t \quad (12)$$

Figures 2 to 5 show $R(t)$ as a function of time for $R_2 = 0.5$ and 0.6 and different flavour numbers ($n_f = 0$ and $n_f = -4$). The straight lines are the behaviour expected with the central value of the splitting that we extract from our data, fitting $R(t)$ to a straight line for $3 < t < t_{\max}$ with $5 \leq t_{\max} \leq 9$. Measurements were taken in a Monte Carlo story consisting of the following basic update procedure, 1 heat bath and 3 overrelaxation steps for the gauge part and 1 heat bath and 10 overrelaxation steps for the fermion part, repeated for a number of sweeps ranging from 23000 to 141000. The errors on the data points are obtained with a standard jackknife algorithm after a binning into clusters of 500 - 1000 measurements. For the pure gauge case, in order to keep the advantage of direct field correlations, we have introduced pseudofermion fields which are thermalized only in a frozen gauge configuration to provide a Monte Carlo inversion of the propagator. In order to reach a sufficient accuracy, the auxiliary system is thermalized for 200 configurations and the correlation measured for 500 more. It has proven useful to introduce many (typically 4) copies of pseudofermion fields in order to increase the number of possible flavour recombinations in the

correlations of currents P_5^{ij} and Q_5^{ij} . The auxiliary fields are introduced also in the one fermion case ($n_f = -2$) to provide additional non dynamical flavours which disentangle eyes from fish diagrams. The results are reported in tables 1 and 2 together with some details on the simulation parameters. Figure 6 and 7 summarize our results and shows m_0 as a function of the flavour number at the two values of criticality that we have explored. The results are consistent with an independence from n_f of m_0 and confirm the validity of the expression of eq. 1. The value of m_0 at $R_2 = 0.5$ is also consistent with another determination obtained in the quenched case [5]. The authors of ref. [5] have explored the value of m_0 at values of quark mass lower than ours. Their extrapolation to the chiral limit leads to a η' mass lower than the experimental value by roughly 10%.

As a further check of the overall picture of singlet meson masses, we have also studied the singlet and non singlet vector meson correlations. In figure 8 the quantity

$$R_V(t) = -\frac{1}{n_f} \log[G_\omega(t)/G_\rho(t)] \quad (13)$$

which is the analogous for vector mesons of $R(t)$, is shown for $n_f = -4$ and $R_2 = 0.5$: it is compatible with zero, indicating that the two states are practically degenerate and confirms the unicity of the pseudoscalar singlet state in QCD.

A last remark concerns the validity of the fermion approach which can be monitored through the value of the η' mass: at large fermion numbers the particle naively speaking becomes massless and may spoil the smoothness of the extrapolations from negative flavour numbers. In all calculations that we have performed, we have used the η' mass as a monitor of the limits of validity of the method.

4 Appendix A

The bermion action is

$$S_b^{(n_b)}[U, \phi^\dagger, \phi] = S_G[U] + \sum_x \sum_{k=1}^{n_b} \phi^{(b)\dagger} Q^2 \phi^{(b)} \quad (14)$$

where ϕ and ϕ^\dagger are commuting fields. For some formal derivations it is useful to introduce an equivalent action

$$S_f^{(-|n_f|)}[U, \tilde{\psi}, \tilde{\psi}^\dagger] = S_G[U] + \sum_{x,y} \sum_{f=1}^{|n_f|} \tilde{\psi}^{(f)\dagger}(x) \gamma_5 Q(x,y) \tilde{\psi}^{(f)}(y) \quad (15)$$

It differs from the standard QCD action only because the $\tilde{\psi}^\dagger$ and $\tilde{\psi}$ fields are commuting variables. We consider in the following a theory with at least two different bermion flavours ($n_f \leq -4$).

The correlation

$$H_{Q^2}(t_x) = \int d^3x \langle Q_5^{ii}(x) Q_5^{jj}(0) \rangle \quad i \neq j \quad (16)$$

can be written, by integrating out the bermion fields, as

$$H_{Q^2}(t_x) = Z^{-1} \int \mathcal{D}U \operatorname{Tr}[\gamma_5 Q_{xx}^{-2}] \operatorname{Tr}[\gamma_5 Q_{00}^{-2}] e^{-S_{eff}[U]} \quad (17)$$

where

$$Z = \int D[U] e^{-S_{eff}^{(n_f)}[U]} \quad (18)$$

and

$$S_{eff}^{(n_f)}[U] = S_G[U] + \frac{|n_f|}{2} \operatorname{Tr}(\log Q^2[U]) \quad (19)$$

Using the relation between the bermion propagator Q_{xy}^{-2} and the fermion propagator M_{xy}^{-1}

$$Q_{xy}^{-2} = \sum_z \gamma_5 M_{xz}^{-1} \gamma_5 M_{zy}^{-1} \quad (20)$$

the correlation $H_{Q^2}(t_x)$ can be written in the form

$$Z^{-1} \int d^3x \int d^4y d^4z \int \mathcal{D}U \operatorname{Tr}[M_{xy}^{-1} \gamma_5 M_{yx}^{-1}] \operatorname{Tr}[M_{0z}^{-1} \gamma_5 M_{z0}^{-1}] e^{-S_{eff}[U]} \quad (21)$$

This expression in terms of pseudofermionic fields $\tilde{\psi}_i$ appears as a four point Green function with two of the four variables integrated over the whole space-time:

$$\int d^3x \int d^4y d^4z \langle 0 | \text{T} [\pi_{12}(y) \sigma_{21}(0) \pi_{34}(z) \sigma_{43}(x)] | 0 \rangle \begin{cases} \pi_{ij} = \tilde{\psi}_i^\dagger \gamma_5 \tilde{\psi}_j \\ \sigma_{ij} = \tilde{\psi}_i^\dagger \tilde{\psi}_j \end{cases} \quad (22)$$

where the $\tilde{\psi}_i$ fields entering the correlation are labelled with a flavour index. The distinction between flavours allows only the contractions represented in eq. 17. Each new flavour has the same mass, a standard propagator M^{-1} , but does not give rise to additional fermion loops and in general it must be considered quenched. However, if $|n_f| \geq 4$, the flavours in eq. 22 can be associated with the dynamical ψ like fields, without introducing additional quenched auxiliary flavours.

The final expression for the continuum case in a infinite volume is obtained by summing over all different time orderings, by inserting complete sets of states in the matrix elements and by using translation invariance. For example the contribution to the integrals in eq. 22 from the region with $0 < t_y < t_z < t_x$ can be written as follows:

$$\sum_{a,b,c} \int d^3x \int d^4y d^4z \theta(t_y) \theta(t_z - t_y) \theta(t_x - t_z) \langle 0 | \sigma_{43}(x) | a, \vec{p}_a \rangle \langle a, \vec{p}_a | \pi_{34}(z) | b, \vec{p}_b \rangle \langle b, \vec{p}_b | \pi_{12}(y) | c, \vec{p}_c \rangle \langle c, \vec{p}_c | \sigma_{21}(0) | 0 \rangle$$

By using translation invariance and by integrating on spatial coordinates this expression reduces to

$$\int dt_y dt_z \theta(t_y) \theta(t_z - t_y) \theta(t_x - t_z) \sum_{a,b,c} e^{-m_a t_x - (m_b - m_a) t_z - (m_c - m_b) t_y} \times \langle 0 | \sigma_{43}(0) | a \rangle \langle a | \pi_{34}(0) | b \rangle \langle b | \pi_{12}(0) | c \rangle \langle c | \sigma_{21}(0) | 0 \rangle$$

where the sum runs only on states with zero spatial momentum. By integrating on t_y and t_z we obtain

$$\sum_{a,b,c} \left\{ \frac{e^{-m_c t_x} - e^{-m_a t_x}}{(m_c - m_a)(m_c - m_b)} - \frac{e^{-m_b t_x} - e^{-m_a t_x}}{(m_c - m_b)(m_b - m_a)} \right\} \times \langle 0 | \sigma_{43}(0) | a \rangle \langle a | \pi_{34}(0) | b \rangle \langle b | \pi_{12}(0) | c \rangle \langle c | \sigma_{21}(0) | 0 \rangle$$

The final result for positive t_x , obtained by considering separately twelve different time ordered contributions, is

$$\int d^3x \int d^4y d^4z \langle 0 | \text{T} [\pi_{12}(y) \sigma_{21}(0) \pi_{34}(z) \sigma_{43}(x)] | 0 \rangle =$$

$$\begin{aligned}
&= \sum_{a,b,c} \left\{ \frac{e^{-m_c t_x} - e^{-m_a t_x}}{(m_c - m_a)(m_c - m_b)} - \frac{e^{-m_b t_x} - e^{-m_a t_x}}{(m_c - m_b)(m_b - m_a)} \right\} \times \\
&\quad \times \langle 0 | \sigma_{43}(0) | a \rangle \langle a | \pi_{34}(0) | b \rangle \langle b | \pi_{12}(0) | c \rangle \langle c | \sigma_{21}(0) | 0 \rangle \\
&+ \frac{e^{-m_b t_x} - e^{-m_c t_x}}{m_a(m_c - m_b)} \langle 0 | \pi_{34}(0) | a \rangle \langle a | \sigma_{43}(0) | b \rangle \langle b | \pi_{12}(0) | c \rangle \langle c | \sigma_{21}(0) | 0 \rangle \\
&+ \frac{e^{-m_a t_x} - e^{-m_b t_x}}{m_c(m_b - m_a)} \langle 0 | \sigma_{43}(0) | a \rangle \langle a | \pi_{34}(0) | b \rangle \langle b | \sigma_{21}(0) | c \rangle \langle c | \pi_{12}(0) | 0 \rangle \\
&+ \frac{e^{-m_c t_x}}{m_a m_b} \langle 0 | \pi_{34}(0) | a \rangle \langle a | \pi_{12}(0) | b \rangle \langle b | \sigma_{43}(0) | c \rangle \langle c | \sigma_{21}(0) | 0 \rangle \\
&+ \frac{e^{-m_a t_x}}{m_c m_b} \langle 0 | \sigma_{43}(0) | a \rangle \langle a | \sigma_{21}(0) | b \rangle \langle b | \pi_{34}(0) | c \rangle \langle c | \pi_{12}(0) | 0 \rangle \\
&+ \frac{e^{-m_b t_x}}{m_a m_c} \langle 0 | \pi_{34}(0) | a \rangle \langle a | \sigma_{43}(0) | b \rangle \langle b | \sigma_{21}(0) | c \rangle \langle c | \pi_{12}(0) | 0 \rangle \\
&+ \{ \pi_{34} \leftrightarrow \pi_{12} \} \tag{23}
\end{aligned}$$

The main difference with respect to the usual correlations is that the parity of the intermediate states is not determined by the one of the operator chosen for the correlation: both parity states contribute because of the insertion of the parity commuter operator $\bar{\psi}\gamma_5\psi$. For large times the lowest lying state dominates. In order to determine which states dominate the correlation at large times we consider a subgroup $SU(2) \times SU(2)$ of the flavour symmetry $SU(|n_f|)$. One $SU(2)$ subgroup is related to isospin transformations on the flavours 1 and 2 while the other $SU(2)$ is the isospin subgroup for flavours 3 and 4. The states which can give non zero contributions to the matrix element products in eq. 23, classified with two isospin numbers and parity, are $(1,0)^\pm$, $(0,1)^\pm$, $(0,0)^\pm$, $(1,1)^\pm$, including both flavoured pions, corresponding to $(1,0)^-$ and $(0,1)^-$, and the $(0,0)^-$ flavour singlet pseudoscalar η' . However a careful examination of eq. 23 shows that the only states whose masses can appear in the exponentially decaying factors are flavour non singlet scalar mesons $(1,0)^+$ and $(0,1)^+$, flavour singlet pseudoscalar $(0,0)^-$ and finally pseudoscalar states $(1,1)^-$ with at least two mesons, while flavoured pions never enter in the exponentials. The conclusion is that, if the η' is lighter then scalar mesons, as is always the case in our simulations, the correlation H_{Q^2} is dominated at large times by this flavour singlet state without contamination from nearest states: the pions.

5 Appendix B

We apply to the berrmions an extension of the “one link integral” technique [7] to derive new berrmionic bilinears, which have the same average value but smaller variance with the respect to the original ones: the meson correlations expressed in terms of these improved bilinears, are found to be correspondingly much more stable.

We define the following two points Green functions:

$$G_{Q^2}(x, y) = \langle Q_5^{ij}(x) Q_5^{ji}(y) \rangle \quad i \neq j \quad (24)$$

$$G_\pi(x, y) = \langle P_5^{ij}(x) P_5^{ji}(y) \rangle \quad i \neq j \quad (25)$$

built from the bilinears defined in eqs. 4 and 5. By integrating over the berrmionic fields one obtains:

$$G_{Q^2}(x, y) = Z^{-1} \int \mathcal{D}U \text{Tr}[Q^{-2}(y, x) \gamma_5 Q^{-2}(x, y) \gamma_5] e^{-S_{eff}[U]} \quad (26)$$

$$G_\pi(x, y) = Z^{-1} \int \mathcal{D}U \text{Tr}[Q^{-1}(y, x) Q^{-1}(x, y)] e^{-S_{eff}[U]} \quad (27)$$

The correlation G_π is equal to the standard pion correlation. In the study of flavour singlet pseudoscalar states (the η' meson) it is also useful to consider the correlations $H(x, y)$ and $H_{Q^2}(x, y)$ defined in eqs 7 and 9. $H(x, y)$ can be written, after integrating on the berrmionic variables, as

$$H(x, y) = Z^{-1} \int \mathcal{D}U \text{Tr}[Q^{-1}(x, x)] \text{Tr}[Q^{-1}(y, y)] e^{-S_{eff}[U]} \quad (28)$$

and it isolates the eye diagram.

We now list the general substitution rules to obtain the berrmionic equivalent of a fermionic bilinear operator. The first is

$$\tilde{\psi} \rightarrow \phi \quad \text{and} \quad \tilde{\psi}^\dagger \rightarrow \phi^\dagger Q \gamma_5 \quad (29)$$

which gives for example the operator $P_5(x)$. The alternative substitution rule

$$\tilde{\psi} \rightarrow Q \phi \quad \text{and} \quad \tilde{\psi}^\dagger \rightarrow \phi^\dagger \gamma_5 \quad (30)$$

gives an equivalent operator

$$\tilde{P}_5^{ij}(x) = \sum_y \phi_i^\dagger(x) Q(x, y) \phi_j(y) \quad (31)$$

Given the bilinears

$$P_5(x) = \tilde{\psi}_x^\dagger \gamma_5 \tilde{\psi}_x \quad (32)$$

$$Q_5(x) = \phi_x^\dagger \gamma_5 \phi_x \quad (33)$$

we define their improved partners¹ where $\Gamma = \gamma_5$:

$$P'_5(x) = a^{-2} [\tilde{\psi}^\dagger (\gamma_5 Q - aI)]_x \Gamma [(\gamma_5 Q - aI) \tilde{\psi}]_x + \frac{N_c}{a} \sum_\alpha \Gamma_{\alpha\alpha} \quad (34)$$

$$Q'_5(x) = A^{-2} (Q^2 \Phi - A\Phi)_x^\dagger \Gamma (Q^2 \Phi - A\Phi)_x + \frac{N_c}{A} \sum_\alpha \Gamma_{\alpha\alpha} \quad (35)$$

$$P''_5(x) = a^{-4} [\tilde{\psi}^\dagger (\gamma_5 Q - aI)^2]_x \Gamma [(\gamma_5 Q - aI)^2 \tilde{\psi}]_x + \frac{N_c}{a^4} \sum_\alpha \Gamma_{\alpha\alpha} \quad (36)$$

$$Q''_5(x) = -A^{-3} (Q^2 \Phi - A\Phi)_x^\dagger \Gamma (Q^4 \Phi - 2AQ^2 \Phi + A^2 \Phi)_x + A^{-3} Tr[Q_{xx}^4 \Gamma] \quad (37)$$

where

$$a = \frac{1}{2\kappa} \quad (38)$$

and

$$A = \frac{1 + 16\kappa^2}{4\kappa^2} \quad (39)$$

The improved operators can replace the original ones with some restrictions on the relative time distance:

$$\langle P_5(x) \rangle = \langle P'_5(x) \rangle = \langle P''_5(x) \rangle \quad (40)$$

$$\langle P'_5(x) P'_5(y) \rangle = \langle P_5(x) P_5(y) \rangle \quad \text{for } |t_y - t_x| \geq 2 \quad (41)$$

$$\langle P''_5(x) P''_5(y) \rangle = \langle P_5(x) P_5(y) \rangle \quad \text{for } |t_y - t_x| \geq 4 \quad (42)$$

and

$$\langle Q_5 \rangle = \langle Q'_5(x) \rangle = \langle Q''_5(x) \rangle \quad (43)$$

¹These definitions are valid for a general bilinear with a spinor matrix Γ .

$$\langle Q'_5(x)Q'_5(y) \rangle = \langle Q_5(x)Q_5(y) \rangle \quad \text{for } |t_y - t_x| \geq 2 \quad (44)$$

$$\langle Q''_5(x)Q''_5(y) \rangle = \langle Q_5(x)Q_5(y) \rangle \quad \text{for } |t_y - t_x| \geq 3 \quad (45)$$

The above relations are obtained by suitable integration of $\tilde{\psi}$ or ϕ fields in single lattice point which leads to their replacement with a function of the surrounding fields.

References

- [1] R. Petronzio, Nucl. Phys. B (Proc. Suppl.) 42 (1995) 942; G. M. de Divitiis, R. Frezzotti, M. Guagnelli, M. Masetti, R. Petronzio, Nucl. Phys. B 455 (1995) 274
- [2] G. M. de Divitiis, R. Frezzotti, M. Guagnelli, M. Masetti, R. Petronzio, Ph. Lett. B 367 (1996) 279; G. M. de Divitiis, R. Frezzotti, M. Masetti, R. Petronzio, preprint ROM2F-96-10, hep-lat/9603020, submitted to Ph. Lett. B; G. M. de Divitiis, R. Frezzotti, M. Masetti, R. Petronzio, preprint ROM2F-96-16, hep-lat/9605002, submitted to Ph. Lett. B
- [3] E. Witten, Nucl. Phys. B 156 (1979) 269
- [4] G. Veneziano, Nucl. Phys. B 159 (1979) 213
- [5] Y. Kuramashi, M. Fukugita, H. Mino, M. Okawa, A. Ukawa, Phys. Rev. Lett. 72 (1994) 3448
- [6] G. M. de Divitiis, R. Frezzotti, M. Guagnelli, M. Masetti, R. Petronzio, Ph. Lett. B 353 (1995) 274
- [7] G. Parisi, R. Petronzio, C. Rapuano, Phys. Lett. B 128 (1983) 418.

n_f	n_{conf}	β	κ	m_π	m_ρ	R_2
-6	23	6.785	0.156	0.477(8)	0.67(1)	0.507(10)
-4	47	6.463	0.158	0.464(4)	0.658(8)	0.497(9)
-2	89	6.1	0.161	0.467(2)	0.662(5)	0.498(5)
0	92	5.7	0.165	0.457(3)	0.659(8)	0.481(7)
-8	30	6.99	0.153	0.563(5)	0.712(10)	0.625(8)
-6	28	6.71	0.1548	0.559(6)	0.716(9)	0.610(8)
-4	45	6.4	0.157	0.552(3)	0.710(6)	0.604(6)
0	31	5.7	0.163	0.562(2)	0.719(4)	0.611(9)

Table 1: The parameters of the simulations, the matched values of π and ρ masses and the number of gauge configurations n_{conf} on which meson correlations are calculated by Dirac operator inversion.

n_f	n_{meas}	β	κ	$\frac{m_{\eta'}-m_\pi}{n_f}$	m_0
-6	23000	6.785	0.156	0.035(7)	0.163(12)
-4	121000	6.463	0.158	0.036(5)	0.168(8)
-2	85×500	6.1	0.161	0.029(8)	0.160(22)
0	90×500	5.7	0.165	0.031(7)	0.167(19)
-8	72000	6.99	0.153	0.0146(31)	0.121(12)
-6	28000	6.71	0.1548	0.0155(60)	0.126(23)
-4	141000	6.4	0.157	0.0167(38)	0.131(14)
0	94×500	5.7	0.163	0.0137(36)	0.124(19)

Table 2: Results for the $\eta' - \pi$ splitting extracted from the ratio $R(t)$. The total number of measurements of the eye correlation $H(t)$ is n_{meas} . For $n_f = 0$ and $n_f = -2$ this correlation was measured 500 times on each fixed gauge configuration. In the quenched case we define $\lim_{n_f \rightarrow 0} \frac{m_{\eta'}-m_\pi}{n_f} = \frac{m_0^2}{2m_\pi}$.

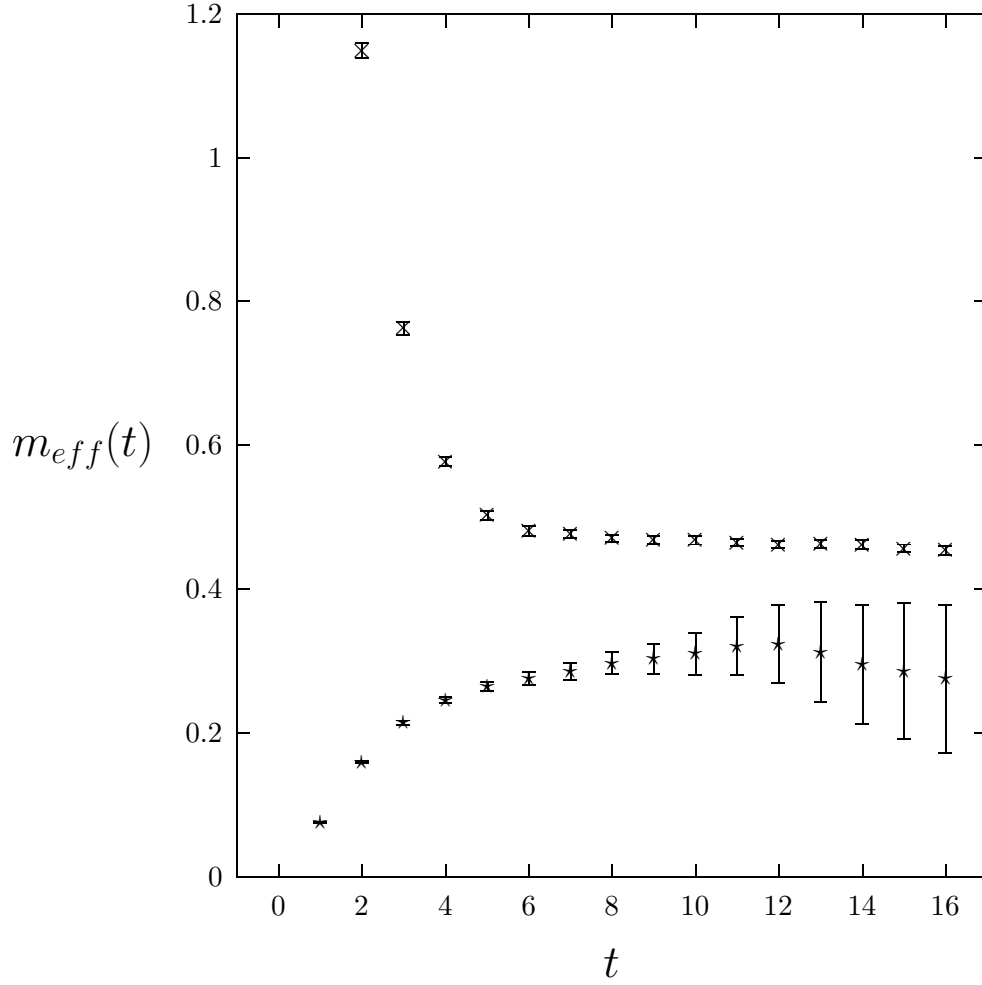


Figure 1: \times : Pion effective mass from the correlation G_π for $n_f = -4$ and $R_2 = 0.5$ (\times); flavour singlet pseudoscalar effective mass from the correlation H_{Q^2} in the same simulation (\star).

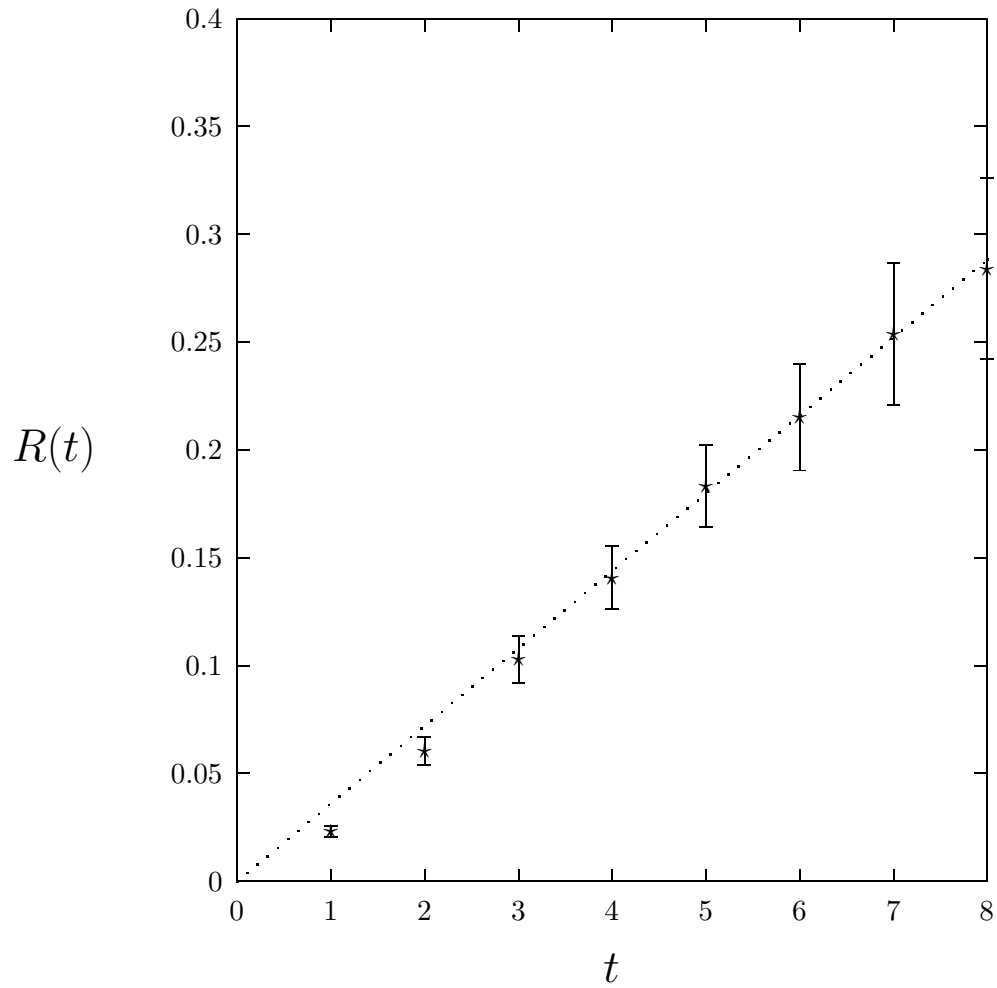


Figure 2: The ratio $R(t)$ for $n_f = -4$; $R_2 = 0.5$.

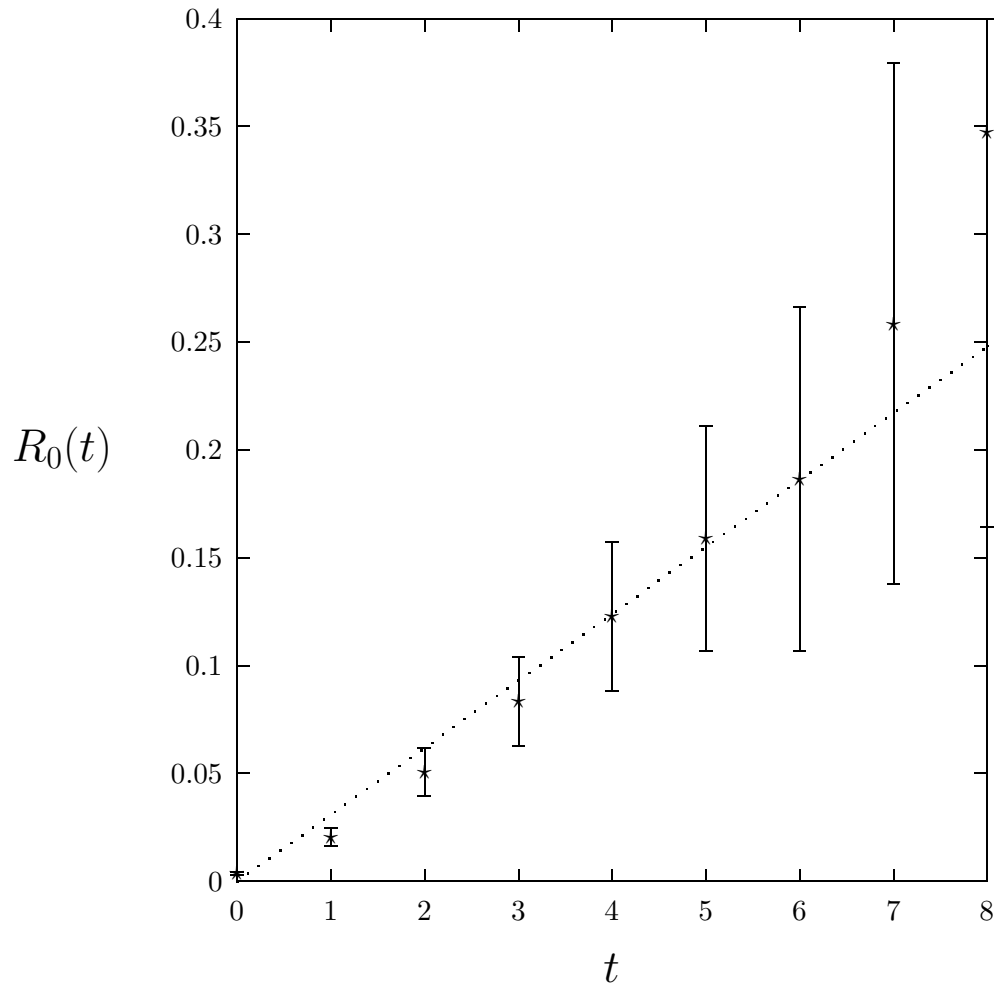


Figure 3: The ratio $R_0(t)$ for $n_f = 0$; $R_2 = 0.5$.

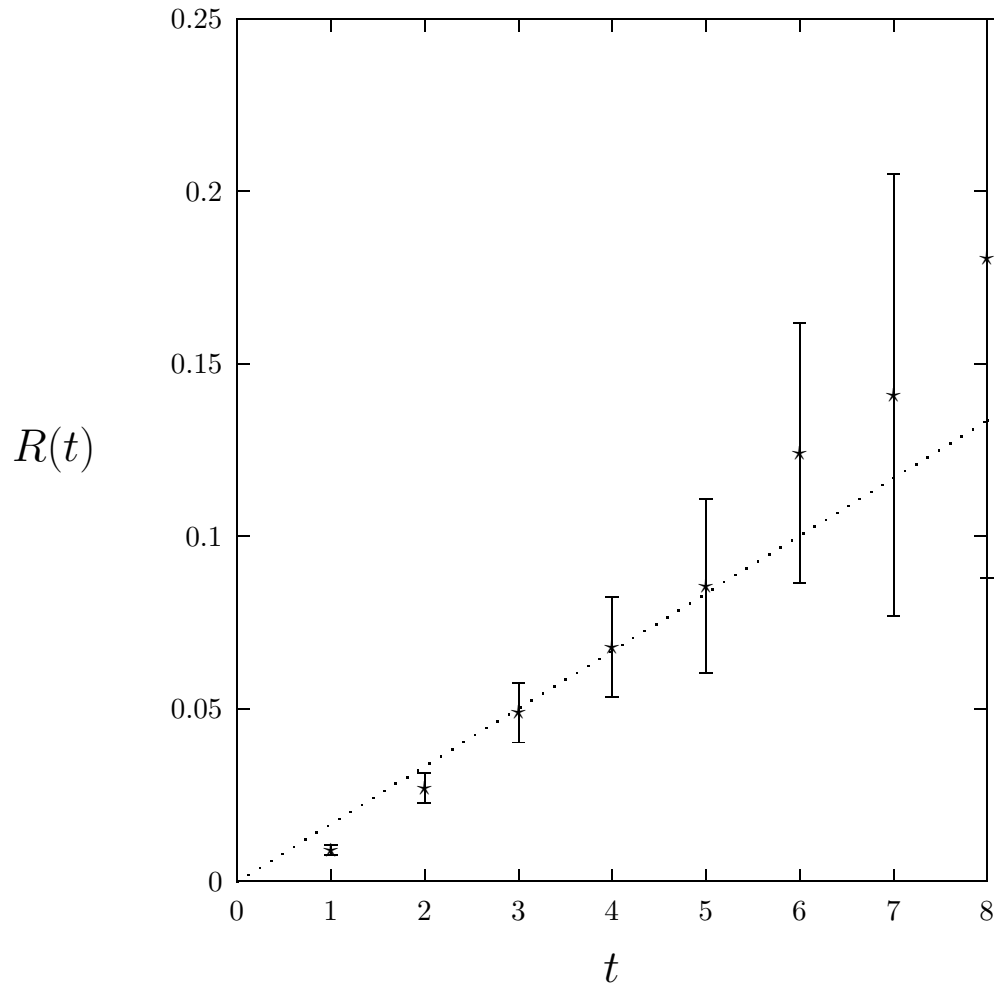


Figure 4: The ratio $R(t)$ for $n_f = -4$; $R_2 = 0.6$.

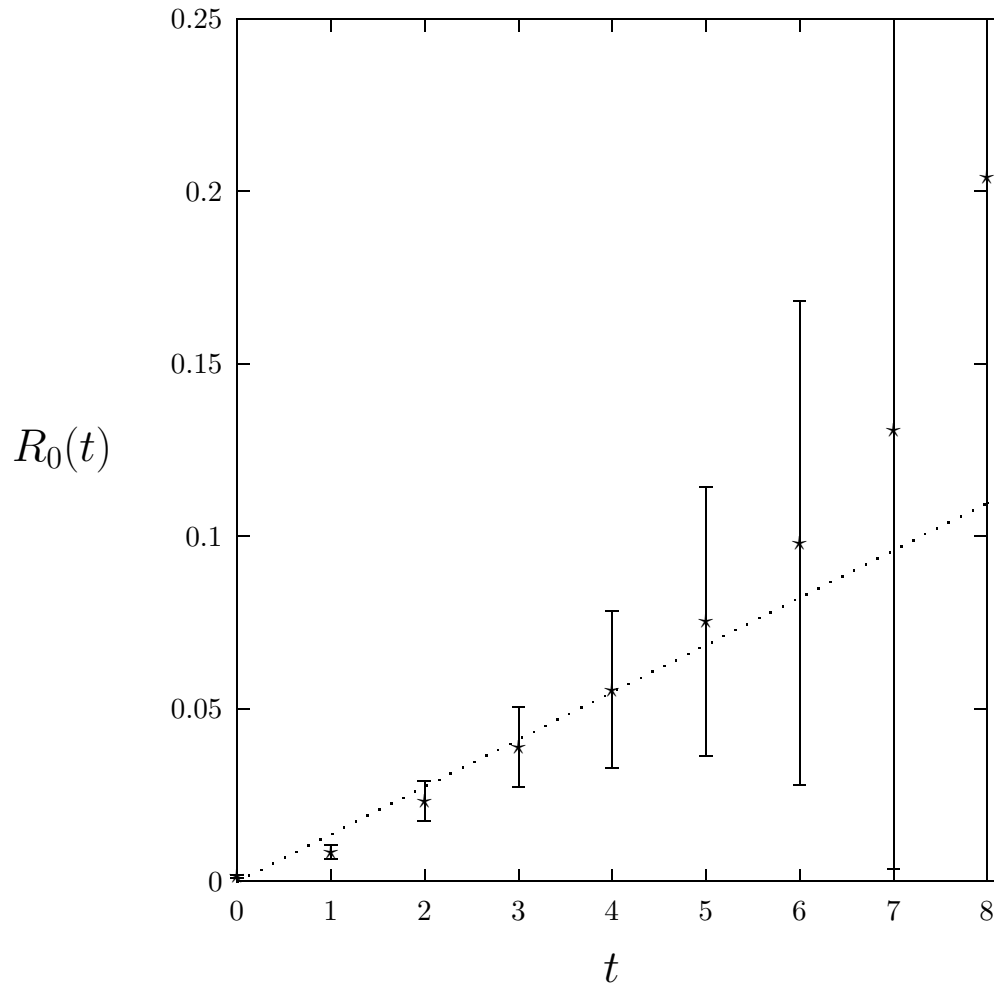


Figure 5: The ratio $R_0(t)$ for $n_f = 0$; $R_2 = 0.6$.

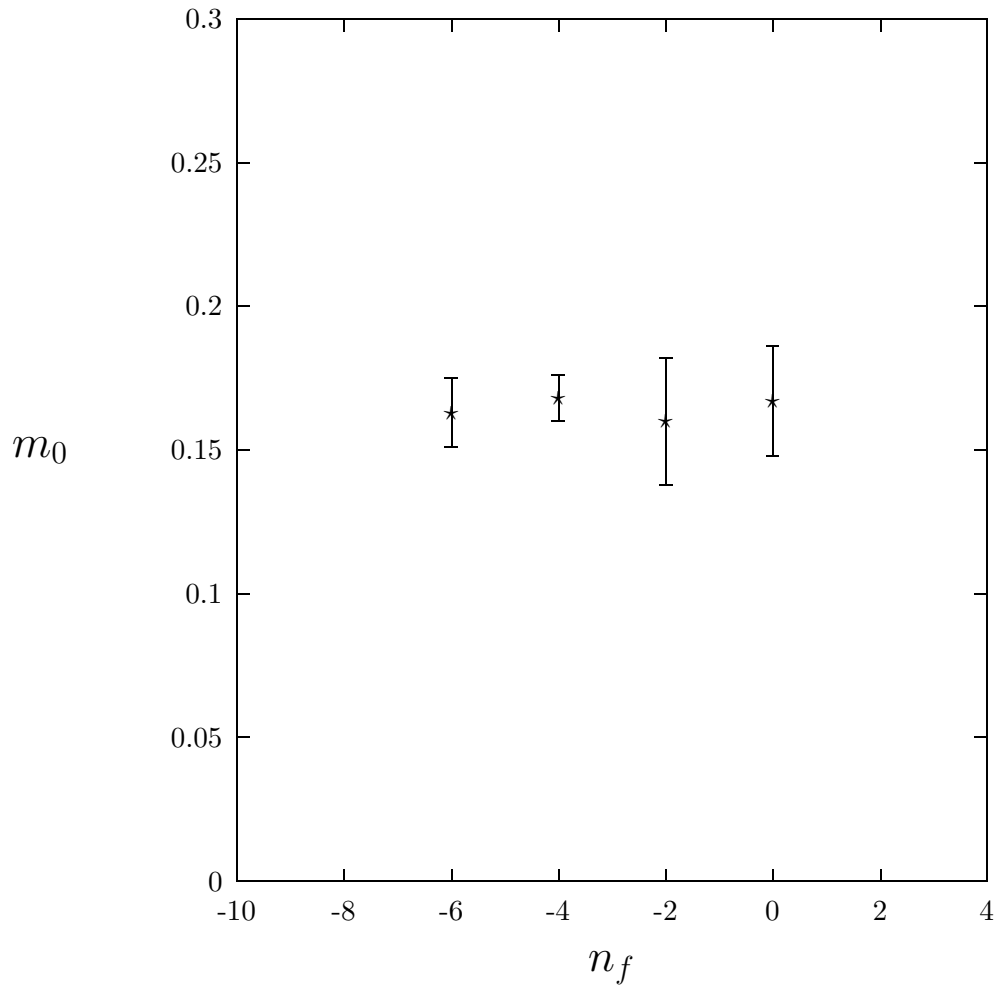


Figure 6: m_0 as a function of n_f for $R_2 = 0.5$.

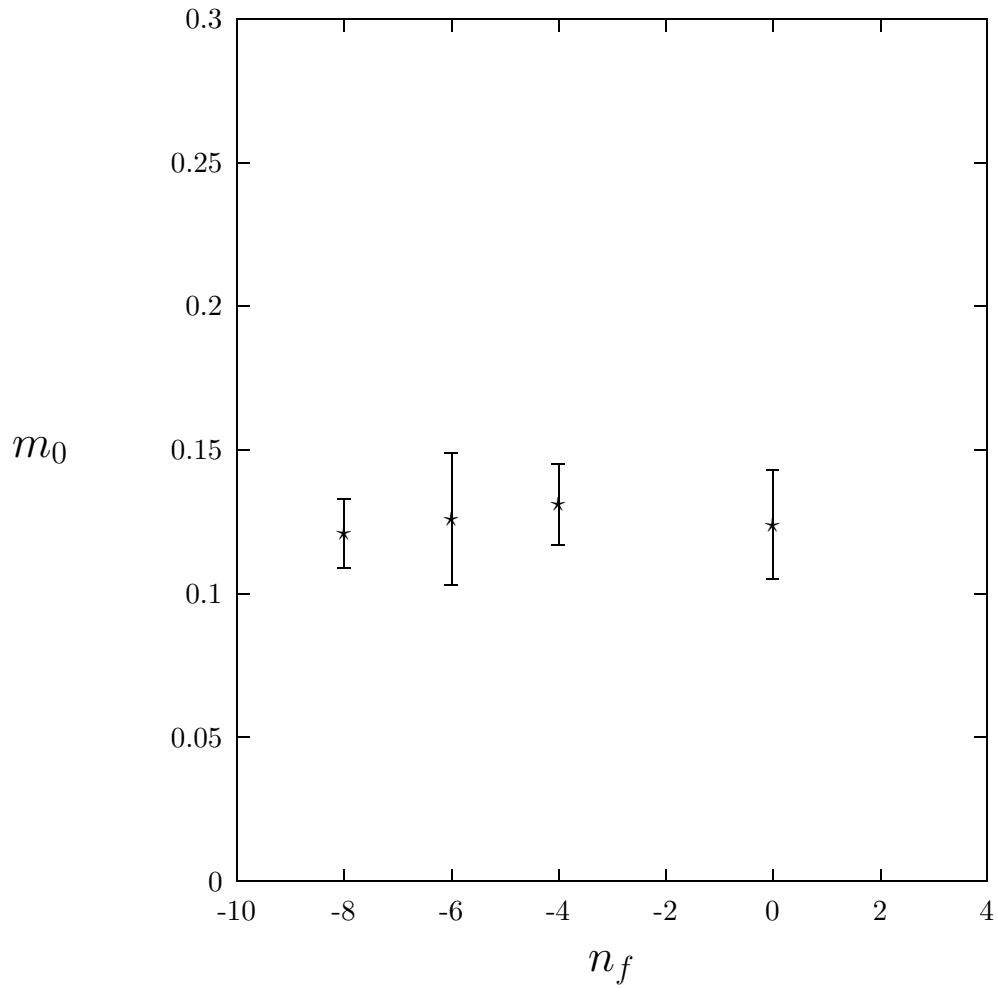


Figure 7: m_0 as a function of n_f for $R_2 = 0.6$.

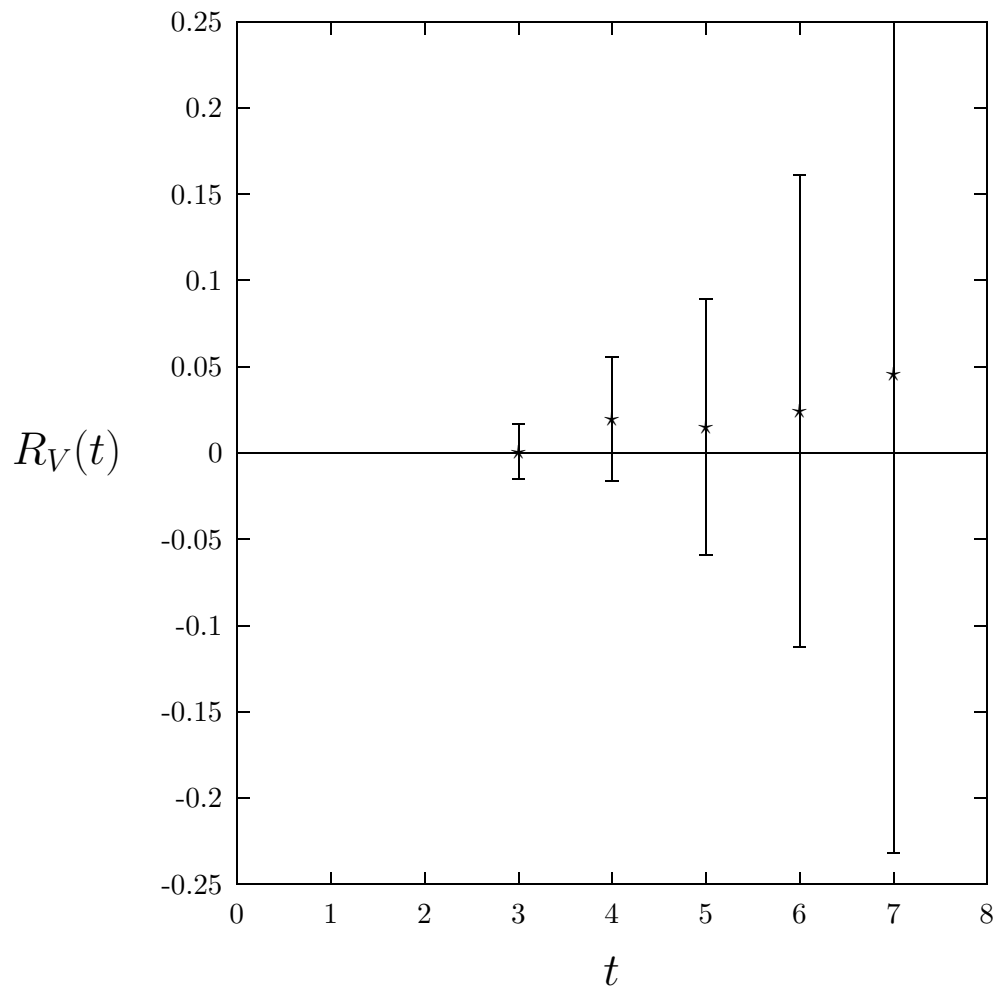


Figure 8: The ratio $R_V(t)$ for $n_f = -4$; $R_2 = 0.5$.